Journal of
Mechanics of
Materials and Structures

ON THE DETACHMENT OF PATCHED PANELS UNDER THERMOMECHANICAL LOADING

William J. Bottega and Pamela M. Carabetta

ON THE DETACHMENT OF PATCHED PANELS UNDER THERMOMECHANICAL LOADING

WILLIAM J. BOTTEGA AND PAMELA M. CARABETTA

The problem of propagation of interfacial failure in patched panels subjected to temperature change and transverse pressure is formulated from first principles as a propagating boundaries problem in the calculus of variations. This is done for both cylindrical and flat structures simultaneously. An appropriate geometrically nonlinear thin structure theory is incorporated for each of the primitive structures (base panel and patch) individually. The variational principle yields the constitutive equations of the composite structure within the patched region and an adjacent contact zone, the corresponding equations of motion within each region of the structure, and the associated matching and boundary conditions for the structure. In addition, the transversality conditions associated with the propagating boundaries of the contact zone and bond zone are obtained directly, the latter giving rise to the energy release rates in self-consistent functional form for configurations in which a contact zone is present as well as when it is absent. A structural scale decomposition of the energy release rates is established by advancing the decomposition introduced in W. J. Bottega, *Int. J. Fract.* **122** (2003), 89–100, to include the effects of temperature. The formulation is utilized to examine the behavior of several representative structures and loadings. These include debonding of unfettered patched structures subjected to temperature change, the effects of temperature on the detachment of beam-plates and arch-shells subjected to three-point loading, and the influence of temperature on damage propagation in patched beam-plates, with both hinged-free and clamped-free support conditions, subjected to transverse pressure. Numerical simulations based on closed form analytical solutions reveal critical phenomena and features of the evolving composite structure. It is shown that temperature change significantly influences critical behavior.

1. Introduction

The role of patched structures has expanded in modern engineering, as uses range from large-scale structural repair to sensors and actuators to small-scale electronic systems. Detachment of the constituent structures is thus an issue of concern as it may influence the effectiveness and integrity of the composite structure. By its nature, the structure possesses a geometrical discontinuity at the edge of the patch. Stress concentrations within the base structure-patch interface at this location (see, for example, [Wang and Rose 2000]) can lead to the initiation of debonding.[1] As a result, a primary mode of failure of such structures under various loading conditions is edge debonding and its propagation. The characterization of edge debonding is thus of critical importance in preserving the useful life of this type of structure.

---

[1]For composite repair of structures, the patch edge is often tapered to discourage debond initiation (see, for example, [Duong and Wang 2007, Chapter 7]). The effect of layer-wise step-tapering on damage propagation was studied in [Bottega and Karlsson 1999] and [Karlsson and Bottega 1999a].

The structures of interest are typically subjected to temperature variations from the reference state. Such temperature changes can influence the onset and extent of damage in these structures. In this light, Duong and Yu [2002] examined the thermal effects of curing on the stress intensity factor for an octahedral-shaped composite repair patch bonded to a cracked rectangular plate. A general expression for the stress distribution was calculated analytically by adopting an "equivalent inclusion method" attributed to Rose [1981], assuming a second order polynomial distribution for the strains. The solution is used to analyze a sample problem and is compared with results using FEM. Related work includes that of Wang et al. [2000], who analyzed thermally-induced residual stresses due to curing in plates with circular patches. Structures were restricted to those with identical coaxial circular patches on the upper and lower faces of the plate so as to eliminate bending as an issue. Moore [2005], with an eye towards avoiding detachment of layers due to uniform temperature change, developed an analytical beam type model in the spirit of Timoshenko [1925] to describe peeling of a composite laminate under thermal load. In this context, he calculated the peeling moment that arises from the peel stress at any interface of the structure due to an applied uniform temperature change from the curing temperature. This was done via a force balance approach, where a decomposition of the moments into thermal and mechanical parts was utilized. The results were then applied to three- and four-layer beams. In a similar vein, Toya et al. [2005] employed a force balance based on classical beam theory to evaluate the energy release rate for a bilayer beam possessing an edge delamination when the structure is subjected to different temperatures at the top surface, bottom surface, and interface. They characterized the mode mix using a small-scale decomposition attributed to Toya [1992] which utilizes complex stress intensity factors and the crack closure method to characterize the energy release rate.

In related work, Karlsson and Bottega [2000a; 2000b] studied the effects of a uniform temperature field applied to a patched plate, where the base structure is fixed at both ends with regard to in-plane translation. In that work, the authors uncovered and explained the instability phenomenon they refer to as "slingshot buckling", whereby, at a critical temperature, the structure "slings" dynamically from an equilibrium configuration possessing deflections in one direction to another equilibrium configuration with deflections in the opposite direction. Rutgerson and Bottega [2002] examined the thermo-elastic buckling of multilayer shell segments. In that study, the layered shells are subjected to an applied transverse pressure in addition to a uniform temperature field. The nonlinear analysis therein showed "slingshot" buckling to occur for thermal loading of these types of structures as well, and at temperatures well below the conventional "limit point" (see also [Rutgerson and Bottega 2004]). The findings on slingshot buckling have since been unified [Bottega 2006]. It is concluded that this type of buckling is inherent to many types of composite structures and occurs due to competing mechanical and thermal elements of the loading. Most recently, Carabetta and Bottega [2008] studied the effects of geometric nonlinearities on the debonding of patched beam-plates subjected to transverse pressure. Analyses using both nonlinear and linearized models were conducted and compared. Significant discrepancies were seen to occur between behaviors predicted by the two models, both with respect to the onset of damage propagation and with regard to the stability of the process and to pre-growth behavior, demonstrating the influence of geometric nonlinearities on the phenomena of interest.

In the present work, we examine debonding of both initially flat and initially curved patched structures under uniform temperature alone and in consort with transverse pressure and three-point loading. Toward this end, the problem of propagation of interfacial debonds in patched panels subjected to temperature

change and transverse pressure is formulated from first principles as a propagating boundaries problem in the calculus of variations, in the spirit of [Bottega 1995; Bottega and Loia 1996; 1997; Bottega and Karlsson 1999; Karlsson and Bottega 1999a; 1999b], where various issues, configurations, and loading conditions were studied. For the present study, temperature is accounted for. A region of sliding contact adjacent to the intact region is also considered, and the boundary of the intact region as well as the boundary between the contact zone and a region of separation of the patch and base panel are each allowed to vary along with the displacements within each region. This is done for both cylindrical and flat structures simultaneously. An appropriate geometrically nonlinear thin structure theory is incorporated for each of the primitive structures (base panel and patch) individually. The variational principle then yields the constitutive equations of the composite structure within the patched region and an adjacent contact zone, the corresponding equations of motion within each region of the structure, and the associated matching and boundary conditions for the structure. In addition, the transversality conditions associated with the propagating boundaries of the contact zone and bond zone are obtained directly, the latter giving rise to the energy release rates in self-consistent functional form for configurations in which a contact zone is present as well as when it is not. A structural scale decomposition of the energy release rates is established by advancing the decomposition of [Bottega 2003] to include the effects of temperature. The formulation is then utilized to examine the behavior of several representative structures and loadings. These include debonding of unfettered patched structures subjected to temperature change, the effects of temperature on the detachment of beam-plates and arch-shells subjected to three-point loading, and the influence of temperature on damage propagation in patched beam-plates, with both hinged-free and clamped-free support conditions, subjected to transverse pressure. (The latter is shown in Figure 1.) Numerical simulations based on exact analytical solutions to the aforementioned formulation are performed, the results of which are presented in load-damage size space. Interpretation of the corresponding "growth paths" admits characterization of the separation behavior of the evolving composite structure. It is shown that temperature change significantly influences critical behavior.

2. Formulation

Consider a thin structure (flat or cylindrical) comprised of a base panel (plate or shell) of normalized half-span L to which a patch of half-span $L_p \leq L$ is adhered over the region $S_1 : s \in [0, a]$ (shown in Figure 2 for a flat panel). The coordinate s runs parallel to the reference surface and originates at the centerspan of the structure, as shown. Further, let us consider the debonded portion of the patch to
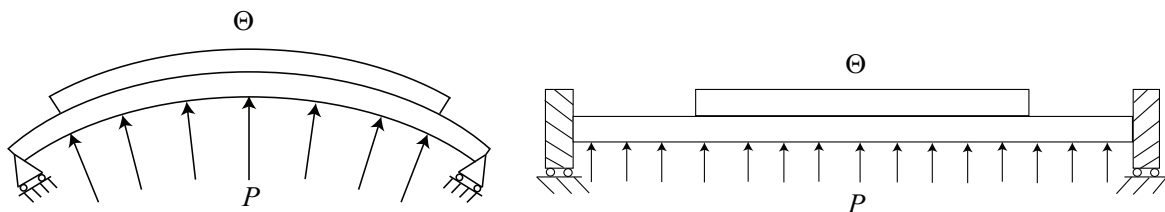

Figure 1. Patched structures subjected to transverse pressure and uniform temperature field. Left: cylindrical panel (arch-shell) with hinged-free supports. Right: flat panel (beam-plate) with clamped-free supports.
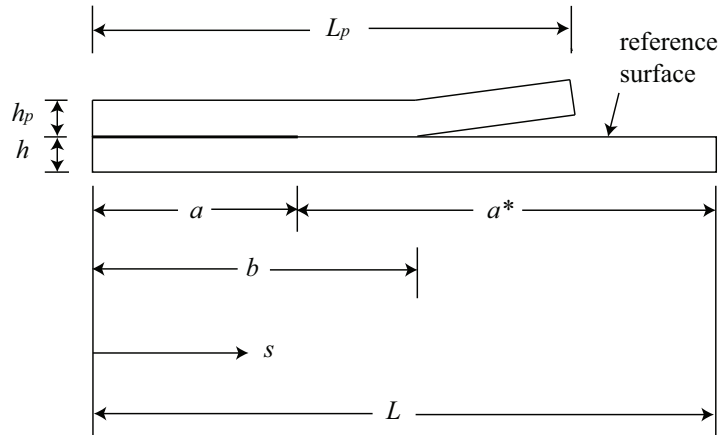
Figure 2. Dimensionless half-span of structure (shown for flat panel).

maintain sliding contact over the region $S_2 : s \in [a, b]$ adjacent to the bonded region, while a portion of the patch defined on $S_3 : s \in [b, L]$ is lifted away from the base structure. These three regions will be referred to as the "bond zone", "contact zone", and "lift zone", respectively. The domain of definition of the portion of the patch within the lift zone is $S_{3p} : s \in [b, L_p]$ such that $S_{3p} \subset S_3$. When referring to the portion of the patch in region S_3 it will be understood that the corresponding subregion is indicated. At this point, let us also define the "conjugate bond zone" $a^* \equiv L - a$ as indicated in the figure. We shall be interested in examining the evolution and response of the composite structure when it is subjected to a uniform temperature increase, Θ, above some reference temperature. In what follows, all length scales are normalized with respect to the dimensional half-span $\bar{L}$ (radius $\bar{R}$) of the undeformed plate (shell) structure, and the common surface or interface between the patch and base panel, and its extension, will be used as the reference surface. The temperature change, Θ, is normalized with respect to the reference temperature (and the coefficient of thermal expansion of the base structure). The corresponding relations for the normalized (centerline) membrane strains $e_i(s)$ and $e_{pi}(s)$ and the normalized curvature changes $\kappa_i(s)$ and $\kappa_{pi}(s)$ for the base structure and the patch in each region are thus given by

$$e_i = u_i' - kw_i + \tfrac{1}{2}w_i'^2, \qquad \kappa_i = w_i'' + kw_i, \qquad (s \in S_i)$$
$$e_{pi} = u_{pi}' - kw_{pi} + \tfrac{1}{2}w_{pi}'^2, \quad \kappa_{pi} = w_{pi}'' + kw_{pi}, \quad (s \in S_{ip})$$
(1)

where $k = 0$ corresponds to the plate and $k = 1$ corresponds to the shell, and the variables are defined as follows: $u_i = u_i(s)$ (positive in the direction of increasing s) and $w_i = w_i(s)$ (positive downward/inward), respectively, correspond to the axial (circumferential) and transverse (radial) displacements of the centerline of the base panel in region S_i, and $u_{pi} = u_{pi}(s)$ and $w_{pi} = w_{pi}(s)$ correspond to the analogous displacements of the centerline of the patch. The primes indicate total differentiation with respect to s.

The displacements $u_i(s)$ and $u_{pi}(s)$, and the membrane strains $e_i(s)$ and $e_{pi}(s)$ of the substructure centerlines are related to their counterparts $u_i^*(s)$ and $u_{pi}^*(s)$, and $e_i^*(s)$ and $e_{pi}^*(s)$ at the reference

surface, by the relations

$$u_i^* = u_i + \tfrac{1}{2}hw_i', \quad u_{pi}^* = u_{pi} - \tfrac{1}{2}h_p w_{pi}' \quad (i = 1, 2, 3)$$
$$e_i^* = e_i + \tfrac{1}{2}h\kappa_i, \quad e_{pi}^* = e_{pi} - \tfrac{1}{2}h_p\kappa_{pi} \quad (i = 1, 2, 3)$$

where $h \ll 1$ is the normalized thickness of the base panel and $h_p \ll 1$ is that of the patch. At this point let us also introduce the normalized membrane stiffness, C, and bending stiffness, D, of the base panel and the corresponding normalized membrane and bending stiffnesses, C_p and D_p, of the patch. The normalization of the stiffnesses of the primitive structures is based on the bending stiffness of the base panel and the half-span $\bar{L}$ (radius $\bar{R}$) of the system in the undeformed configuration. Hence,

$$C = 12/h^2, \qquad D = 1, \qquad C_p = CE_0 h_0, \qquad D_p = E_0 {h_0}^3, \tag{2}$$

where $h_0 = h_p/h$, and

$$E_0 = \bar{E}_p/\bar{E} \quad \text{(plane stress)} \qquad \text{or} \qquad E_0 = \frac{\bar{E}_p/(1 - v_p^2)}{\bar{E}/(1 - v^2)} \quad \text{(plane strain)},$$

where $\bar{E}$ and $\bar{E}_p$ correspond to the (dimensional) elastic moduli of the base panel and patch, respectively, and v and v_p are the associated Poisson's ratios.

The nondimensional coefficients of thermal expansion of the base structure and patch, α^0 and α_p^0, respectively, are the products of the dimensional coefficients and the reference temperature. We correspondingly define, for the present formulation, the augmented coefficients α and α_p such that

$$\alpha = \alpha^0 \qquad \text{and} \quad \alpha_p = \alpha_p^0 \qquad \text{(plane stress)},$$
$$\alpha = (1 + v)\alpha^0 \quad \text{and} \quad \alpha_p = (1 + v_p)\alpha_p^0 \qquad \text{(plane strain)}. \tag{3}$$

We next introduce the normalized temperature scale, Θ, such that

$$\tilde{\Theta} = \alpha\Theta = \alpha\frac{\bar{\Theta} - \bar{\Theta}_0}{\bar{\Theta}_0}, \tag{4}$$

where $\bar{\Theta}$ is the dimensional temperature and $\bar{\Theta}_0$ is a reference temperature.

Paralleling the developments in [Bottega 1995], we next formulate an energy functional in terms of (i) the strain energies of each of the individual segments of both the base panel and patch, independently, and expressed in terms of the reference surface variables, (ii) the work done by the applied loading for each case of interest, (iii) constraint functionals which match the transverse displacements in the contact zone and both the transverse (radial) and in-plane (circumferential) displacements in the bond zone[2], and (iv) a delamination energy functional corresponding to the energy required to create a unit length of new disbond. To complete the formulation, we include a thermal energy functional. We thus formulate the energy functional Π as follows:

$$\Pi = \sum_{i=1}^{3} \left(U_B^{(i)} + U_{Bp}^{(i)} + U_M^{(i)} + U_{Mp}^{(i)} + U_T^{(i)} + U_{Tp}^{(i)} \right) - \Lambda - \mathcal{W} + \Gamma, \tag{5}$$

---

[2]The Lagrange multipliers in this case correspond to the interfacial normal and shear stresses, respectively.

where

$$U_B^{(i)} = \int_{S_i} \tfrac{1}{2} D\kappa_i^2 \, ds, \quad \text{and} \quad U_{Bp}^{(i)} = \int_{S_i} \tfrac{1}{2} D_p \kappa_{pi}{}^2 \, ds \quad (i = 1, 2, 3), \tag{6}$$

correspond to the bending energies in the base panel and the patch in region S_i, while

$$U_M^{(i)} = \int_{S_i} \tfrac{1}{2} C(e_i - \alpha\Theta)^2 \, ds \quad \text{and} \quad U_{Mp}^{(i)} = \int_{S_i} \tfrac{1}{2} C_p (e_{pi} - \alpha_p\Theta)^2 \, ds \quad (i = 1, 2, 3)$$

are the corresponding stretching energies of the base panel and the patch. Further,

$$U_T^{(i)} = \int_{S_i} \left(c_\sigma - (1 + \Theta)c_e \right)\Theta \, ds, \quad U_{Tp}^{(i)} = \int_{S_i} \left(c_{\sigma p} - (1 + \Theta)c_{ep} \right)\Theta \, ds$$

represent the "thermal energies" of the base structure and the patch, respectively, such that the total bracketed expression in (5) corresponds to the (Helmholtz) free energy of the structure, and Θ is the normalized temperature change. The quantities c_σ, c_e ($c_{\sigma p}$, c_{ep}) correspond to the normalized specific heats of the base structure (patch) for constant stress and constant deformation, respectively. These terms are included for completeness. We remark that since we shall consider the normalized temperature change, Θ, as prescribed, the variation of these functionals will vanish identically. (The contribution of the convective type terms of these particular functionals for a given region, associated with the propagation of the interior boundaries $s = a$ and $s = b$, will cancel and hence will have no contribution to the overall variation of Π as well.) Further, if the process is considered to be adiabatic, these terms will vanish identically as the free energy goes to internal energy and may be interpreted as the adiabatic work given by the first four functionals.

The functional Λ appearing in (5) is a constraint functional given by

$$\Lambda = \sum_{i=1}^{2} \int_{S_i} \sigma_i (w_{pi} - w_i) \, ds + \int_{S_i} \tau (u_{p1}^* - u_1^*) \, ds,$$

where σ_1, σ_2 and τ are Lagrange multipliers (and $\sigma_2 < 0$). Further,

$$\mathcal{W} = -\sum_{i=1}^{3} \int_{S_i} p w_i \, ds$$

is the work done by the applied pressure, and

$$\Gamma = 2\gamma(a^* - a_0^*)$$

is the delamination energy[3], where

$$a^* = L - a$$

is the conjugate bond zone half-length as defined earlier, a_0^* corresponds to some initial value of a^*, and γ is the normalized bond energy (bond strength).

The normalized bond energy, γ, is related to its dimensional counterpart, $\bar{\gamma}$, by the relations

$$\gamma = \bar{\gamma}\bar{\ell}^2/\bar{D},$$

---

[3]More generally, γ may be considered to be an implicit function of a^*. In this event, the functional Γ is defined in terms of its first variation, $\delta\Gamma = 2\gamma\delta a^*$ (that is, the virtual work of the generalized force γ).

where $\bar{D}$ is the dimensional bending stiffness of the base panel and $\bar{\ell} = \bar{L}, \bar{R}$ (plate, shell). Likewise, the normalized interfacial stresses σ_1, σ_2, and τ (the Lagrange multipliers), and the normalized applied pressure p, are related to their dimensional counterparts $\bar{\sigma}_1, \bar{\sigma}_2, \bar{\tau}$, and $\bar{p}$, respectively, by

$$\sigma_i = \bar{\sigma}_i \bar{\ell}^3 / \bar{D} \quad (i = 1, 2), \qquad \tau = \bar{\tau} \bar{\ell}^3 / \bar{D}, \, p = \bar{p} \bar{\ell}^3 / \bar{D}.$$

We next invoke the principle of stationary potential energy which, in the present context, is stated as

$$\delta \Pi = 0.$$

Taking the appropriate variations, allowing the interior boundaries a and b to vary along with the displacements, we arrive at the corresponding differential equations, boundary and matching conditions, and *transversality conditions* (the conditions that establish values of the "moveable" interior boundaries a and b to be found as part of the solution, together with the associated displacement field, which correspond to equilibrium conditions of the evolving structure). After eliminating the Lagrange multipliers from the resulting equations, we arrive at a self-consistent set of equations and conditions (including the energy release rates) for the evolving composite structure. We thus have

$$M_i^{*''} + k(M_i^* - N_i^*) - (N_i^* w_i^{*'})' = -p, \qquad N_i^{*'} = 0 \qquad (s \in S_i; \, i = 1, 2) \tag{7}$$

$$M_3'' + k(M_3 - N_3) - (N_3 w_3')' = -p, \qquad N_3' = 0 \qquad (s \in S_3) \tag{8}$$

$$M_{p3}'' + k(M_{p3} - N_{p3}) - (N_{p3} w_{p3}')' = 0, \qquad N_{p3}' = 0 \qquad (s \in S_{3p}) \tag{9}$$

with

$$w_i^*(s) \equiv w_i(s) = w_{pi}(s) \qquad (s \in S_i; \, i = 1, 2),$$

$$\kappa_i^*(s) \equiv \kappa_i(s) = \kappa_{pi}(s) \qquad (s \in S_i; \, i = 1, 2),$$

$$u_1^*(s) = u_{p1}^*(s) \qquad (s \in S_1).$$

Here

$$N_i(s) = C[e_i(s) - \alpha\Theta], \qquad N_{pi}(s) = C_p[e_{pi}(s) - \alpha_p\Theta] \qquad (i = 1, 2, 3)$$

are the normalized resultant membrane forces acting on a cross section of the base panel and patch within region S_i $(i = 1, 2, 3)$;

$$N_1^*(s) = C^* e_1^*(s) + B^* \kappa_1^*(s) - n^*\Theta = C^*[e_1^*(s) - \alpha^*\Theta] + B^*[\kappa_1^*(s) - \beta^*\Theta], \tag{10}$$

$$M_1^*(s) = A^* \kappa_1^*(s) + B^* e_1^*(s) - \mu^*\Theta = A^*[\kappa_1^*(s) - \beta^*\Theta] + B^*[e_1^*(s) - \alpha^*\Theta] \tag{11}$$

$$= D^*[\kappa_1^*(s) - \beta^*\Theta] + \rho^* N_1^*,$$

respectively, correspond to the normalized membrane force and normalized bending moment acting on a cross section of the bonded portion of the composite structure;

$$N_2^*(s) = N_2 + N_{p2} \quad \text{and} \quad M_2^*(s) = D_c \kappa_2^*(s) + \tfrac{1}{2}(h_p N_{p2} - h N_2) \tag{12}$$

correspond to the normalized resultant membrane force and bending moment for the debonded portion of the composite structure within the contact zone; and

$$M_3(s) = D\kappa_3(s) - \tfrac{1}{2}hN_3 \quad \text{and} \quad M_{p3}(s) = D_p \kappa_{p3}(s) + \tfrac{1}{2}h_p N_3,$$

correspond to the normalized bending moments in the base panel and patch segments within the region of separation (or lift zone).

The stiffnesses and thermal coefficients of the composite structure defined by (10), (11), and (12) are found in terms of the stiffnesses and thicknesses of the primitive substructures as

$$A^* = D + D_p + (h/2)^2 C + (h_p/2)^2 C_p, \qquad B^* = (h_p/2)C_p - (h/2)C,$$

$$C^* = C + C_p, \qquad\qquad\qquad D^* = A^* - \rho^* B^* = D_c + (h^*/2)^2 C_s, \qquad (13)$$

$$\alpha^* = \alpha_1 - \rho^* \beta^*, \qquad\qquad\qquad \beta^* = m^*/D^*,$$

where

$$\rho^* = B^*/C^*, \qquad\qquad D_c = D + D_p, \qquad h^* = h + h_p, \qquad C_s = C C_p/C^*,$$
$$\mu^* = \tfrac{1}{2} h_p C_p \alpha_p - \tfrac{1}{2} h C \alpha, \quad n^* = C_p \alpha_p + C \alpha, \quad m^* = \mu^* - \rho^* n^*, \quad \alpha_1 = n^*/C^*. \qquad (14)$$

The quantity ρ^* is seen to give the transverse (radial) location of the centroid of the composite structure with respect to the reference surface, D_c is the bending stiffness of the debonded segment of the composite structure in the contact zone, $h^* \ll 1$ is the normalized thickness of the composite structure, and C_s is an effective (series) membrane stiffness. In addition, the parameters α^* and β^* are seen to correspond to the thermal expansion coefficients of the intact portion of the composite structure, and correspond to the thermally-induced membrane strain at the reference surface and the associated curvature change, respectively, per unit normalized temperature change for a free unloaded structure. The thermal expansion coefficient α_1 is seen to be the corresponding strain per unit temperature at the centroid of the intact segment of an unloaded composite structure.

The associated boundary and matching conditions are obtained similarly:

$$u_1^*(0) = 0, \qquad w_1^{*\prime}(0) = 0, \qquad [M_1^{*\prime} - N_1^* w_1^{*\prime}]_{s=0} = 0 \qquad \text{(symmetric deformation)} \quad (15a)$$

$$u_0^*(0) \equiv u_1^*(0) + \rho^* w_1^{*\prime}(0) = 0, \qquad w_1^*(0) = 0, \quad \kappa_1^*(0) = 0 \qquad \text{(antisymmetric deformation)} \quad (15b)$$

$$u_1^*(a) = u_2^*(a) = u_{p2}^*(a), \qquad N_1^*(a) = N_2^*(a) \qquad\qquad (a = a_L, -a_R) \quad (16)$$

$$w_1^*(a) = w_2^*(a), \qquad w_1^{*\prime}(a) = w_2^{*\prime}(a) \qquad\qquad (a = a_L, -a_R) \quad (17)$$

$$[M_1^{*\prime} - N_1^* w_1^{*\prime}]_{s=a} = [M_2^{*\prime} - N_2^* w_2^{*\prime}]_{s=a}, \quad M_1^*(a) = M_2^*(a) \qquad (a = a_L, -a_R) \quad (18)$$

$$u_2^*(b) = u_3^*(b), \qquad\qquad N_2(b) = N_3(b) \qquad\qquad (b = b_L, -b_R) \quad (19)$$

$$u_{p2}^*(b) = u_{p3}^*(b), \qquad\qquad N_{p2}(b) = N_{p3}(b) \qquad\qquad (b = b_L, -b_R) \quad (20)$$

$$w_2^*(b) = w_3(b) = w_{p3}(b), \qquad w_2^{*\prime}(b) = w_3'(b) = w_{p3}'(b) \quad (b = b_L, -b_R) \quad (21)$$

$$M_2^*(b) = M_3(b) + M_{p3}(b) \qquad\qquad (b = b_L, -b_R) \quad (22)$$

$$[M_2^{*\prime} - N_2^* w_2^{*\prime}]_{s=b} = [M_3' - N_3 w_3']_{s=b} + [M_{p3}' - N_{p3} w_{p3}']_{s=b} \qquad (b = b_L, -b_R) \quad (23)$$

$$N_{p3}(\pm L_p) = \kappa_{p3}(\pm L_p) = [M_{p3}' - N_{p3} w_{p3}']_{s=\pm L_p} = 0 \qquad (24)$$

$$u_3(\pm L) = 0 \qquad \text{or} \qquad N_3(\pm L) = 0 \qquad (25)$$

$$w_3'(\pm L) = 0 \qquad \text{or} \qquad \kappa_3(\pm L) = 0 \qquad (26)$$

$$w_3(\pm L) = 0 \qquad (27)$$

The transversality condition for the propagating bond zone boundaries, $a = a_L, -a_R$, with the associated propagating contact zone boundaries, $b = b_L, -b_R$, take the following forms depending upon the presence or absence of a contact zone:

$$\mathcal{G}^{(2)}\{a\} = 2\gamma \quad (b > a), \qquad \mathcal{G}^{(3)}\{a\} = 2\gamma \quad (b = a). \tag{28}$$

In these expressions, the quantities

$$\mathcal{G}^{(i)}\{a\} \equiv G_{MM}^{(i)} + G_{MT}^{(i)} + G_{TM}^{(i)} + G_{TT} \quad (i = 2, 3)$$

are the energy release rates, whose components are given by

$$G_{MM}^{(2)} \equiv \left[\tfrac{1}{2} D_c \kappa_2^{*2} + \tfrac{1}{2C} N_2^2 + \tfrac{1}{2C_p} N_{p2}^2\right]_{s=a} - \left[\tfrac{1}{2} D^*(\kappa_1^* - \beta^*\Theta)^2 + \tfrac{1}{2C^*} N_1^{*2}\right]_{s=a}, \tag{29}$$

$$G_{MM}^{(3)} \equiv \left[\tfrac{1}{2} D \kappa_3^2 + \tfrac{1}{2} D_p \kappa_{p3}^2 + \tfrac{1}{2C} N_3^2 + \tfrac{1}{2C_p} N_{p3}^2\right]_{s=a} - \left[\tfrac{1}{2} D^*(\kappa_1^* - \beta^*\Theta)^2 + \tfrac{1}{2C^*} N_1^{*2}\right]_{s=a}, \tag{30}$$

$$G_{MT}^{(i)} \equiv \left[\tfrac{1}{2} N_i e_T + \tfrac{1}{2} N_{pi} e_{pT}\right]_{s=a} - \left[\tfrac{1}{2} N_1^* e_T^* + \tfrac{1}{2} M_1^* \kappa_T^*\right]_{s=a} \quad (i = 2, 3), \tag{31}$$

$$G_{TM}^{(i)} \equiv \left[\tfrac{1}{2} N_T e_{pi}^\circ + \tfrac{1}{2} N_{pT} e_i^\circ\right]_{s=a} - \left[\tfrac{1}{2} N_T^* e_0^* + \tfrac{1}{2} M_T^* \kappa_0^*\right]_{s=a} \quad (i = 2, 3), \tag{32}$$

$$G_{TT} \equiv \left[\tfrac{1}{2} N_T e_T + \tfrac{1}{2} N_{pT} e_{pT}\right]_{s=a} - \left[\tfrac{1}{2} N_T^* e_T^* + \tfrac{1}{2} M_T^* \kappa_T^*\right]_{s=a}, \tag{33}$$

where the following measures have been introduced:

$$e_i^\circ \equiv e_i - \alpha\Theta, \qquad e_{pi}^\circ \equiv e_{pi} - \alpha_p\Theta \qquad (i = 2, 3), \tag{34}$$

$$e_T \equiv \alpha\Theta, \qquad e_{pT} = \alpha_p\Theta, \qquad N_T = C\alpha\Theta, \qquad N_{pT} = C_p\alpha_p\Theta, \tag{35}$$

$$e_0^* \equiv e_1^* - \alpha^*\Theta, \qquad \kappa_0^* \equiv \kappa_1^* - \beta^*\Theta, \qquad e_T^* \equiv \alpha^*\Theta, \qquad \kappa_T^* \equiv \beta^*\Theta, \tag{36}$$

$$N_T^* \equiv C^*\alpha_1\Theta = C^* e_T^* + B^*\kappa_T^*, \qquad M_T^* \equiv \mu^*\Theta = D^*\kappa_T^* + \rho^* N_T^*. \tag{37}$$

The conditions established by those equations suggest the following *delamination criterion*:

If, for some initial value $a = a_0$ of the bond zone boundary, the state of the structure is such that $\mathcal{G}^{(i)}\{a\} \geq 2\gamma$, then delamination growth occurs and the system evolves (a decreases, a^* increases) in such a way that the corresponding equality in (28) is satisfied. If $\mathcal{G}^{(i)}\{a\} < 2\gamma$, delamination growth does not occur.

For a propagating contact zone ($s = b$), the associated transversality condition reduces to the form

$$\kappa_2^*(b) = \kappa_3(b) = \kappa_{p3}(b) \qquad (b = b_L < L_p, -b_R > -L_p), \tag{38}$$

to which we add the qualification

$$\kappa_3(b^+) > \kappa_{p3}(b^+) \tag{39}$$

in order to prohibit penetration of the base panel and patch for $s \in S_{3p}$. It is thus seen that such a boundary is defined by the point where the curvature changes of the respective segments of the structure are continuous.

The equations introduced so far define the class of problems of interest.

The boundary conditions (24), together with (9), indicate that the "flap" (the segment of the debonded portion of the patch that is lifted away from the base structure) is unloaded, and hence that

$$N_{p3}(s) = \kappa_{p3}(s) = M'_{p3}(s) = 0 \qquad (s \in S_{3p}). \qquad (40)$$

Further, integration of $(7)_2$ and $(8)_2$, imposition of the associated matching conditions stated by $(16)_3$, $(19)_2$, and $(20)_2$, and incorporation of $(40)_1$ yield the results that

$$N_1^* = N_2 = N_3 = N_0 = \text{ constant}, \qquad N_{p2} = 0. \qquad (41)$$

The remaining equations are modified accordingly, with the transversality conditions stated in (28) and (38) taking the forms

$$\left.\begin{array}{l} \mathcal{G}^{(2)}\{a\} \longrightarrow \left[\frac{1}{2}D_c\kappa_2^{*2} - \frac{1}{2}D^*\kappa_1^{*2} + \frac{1}{2}N_0^2/C_e + N_0(\alpha-\alpha_1)\Theta + \frac{1}{2}\eta\Theta^2\right]_{s=a} = 2\gamma \quad (b > a) \\[2mm] \mathcal{G}^{(3)}\{a\} \longrightarrow \left[\frac{1}{2}D\kappa_3^2 - \frac{1}{2}D^*\kappa_1^{*2} + \frac{1}{2}N_0^2/C_e + N_0(\alpha-\alpha_1)\Theta + \frac{1}{2}\eta\Theta^2\right]_{s=a} = 2\gamma \quad (b = a) \end{array}\right\} \qquad (42)$$

and

$$\kappa_2^*(b) = \kappa_3(b) = 0, \qquad \kappa_3(b^+) > 0 \qquad (b < L_p), \qquad (43)$$

where

$$\frac{1}{C_e} \equiv \frac{C_p/C}{C^*}, \qquad \eta \equiv \alpha^2 C + \alpha_p^2 C_p - \alpha_1^2 C^*. \qquad (44)$$

It may be seen from (43) that a propagating or intermediate contact zone boundary may occur only if conditions are such that an inflection point or pseudo-inflection point occurs on the interval $a < s < L_p$. If not, the system will possess either a full contact zone ($b = L_p$), or no contact zone ($b = a$). For the former case, the lifted segment of the flap (region S_{3p}) will not exist and the condition

$$\kappa_2(a^+) < 0 \qquad (b = L_p) \qquad (45)$$

must be satisfied.

Integrating the strain-displacement relations and imposing the boundary and matching conditions for the axial (circumferential) displacements results in the following *integrability condition*:

$$u_3(L) - u_0 = N_0\left(\frac{a^*}{C} + \frac{a}{C^*}\right) + (a^*\alpha + a\alpha_1)\Theta - \left(\frac{h}{2} + \rho^*\right)w'(a) + \sum_{i=1}^{3}\int_{S_i}\left(k(1-\rho^*\delta_{i1})w_i - \frac{1}{2}w_i'^2\right)ds, \qquad (46)$$

where

$$u_0 \equiv [u_1^* + \rho^* w_1']_{s=0} \qquad (47)$$

is the axial (circumferential) deflection of the neutral surface of the composite structure at the origin, and δ_{ij} is Kronecker's delta. The counterparts of $(7)_1$ and $(8)_1$ and the corresponding boundary and matching conditions obtained upon substitution of (38)–(40), together with the transversality conditions stated in (42) and (43), and the integrability condition, (46), transform the problem statement into a *mixed formulation* in terms of the transverse displacements $w_i(s)$ ($i = 1, 2, 3$), the membrane force N_0, and the moving boundaries a and b.

3. Delamination mode mix

The bond energy (that is, interfacial toughness) is generally dependent upon the mix of "delamination modes". To assess this influence for the system under consideration, we adopt the structural scale decomposition of the energy release rate for long thin-layered structures established by Bottega [2003] and extend it to include the thermal effects considered for the present study. In the aforementioned reference, the decomposition is established for a general structure and is then applied to selected specific structural configurations, including patched structures. The presence of a contact zone is taken to imply pure mode-II delamination, while the absence of contact is considered to (generally) imply mixed mode-I and mode-II delamination. The mixed mode decomposition is based on the energy release rates for contact and no contact together with a "curvature of contact" defined therein. The decomposition for the present problem follows directly from the aforementioned reference and the inclusion of the thermal terms as follows. The last three terms of the energy release rates given by (42) are seen to constitute the relative thermomechanical membrane energy at the bond zone boundary and thus contribute to the mode-II delamination energy release rate. Incorporating the last two of these (the first is already included in the original) into the resulting partitioning of the energy release rate for the class of patched structures currently under consideration [Bottega 2003, Section 5.3] gives the following decomposition for the present structure:

$$G_I = \tfrac{1}{2} D_I \kappa_3^2(a), \quad G_{II} = \tfrac{1}{2}\big[D_{II}\kappa_3^2 - D^*\kappa_1^{*2}\big]_{x=a} + \big(\tfrac{1}{2}N_0^2/C_e + N_0(\alpha - \alpha_1)\Theta + \tfrac{1}{2}\eta\Theta^2\big), \quad (48)$$

where G_I and G_{II} are, respectively, the mode-I (opening mode) and mode-II (sliding mode) energy release rates, and

$$D_I = D_p D/D_c, \qquad D_{II} = D^2/D_c. \tag{49}$$

The mode ratio G_{II}/G_I can be readily evaluated using (48) for any configuration determined by the formulation established in this section.

4. Analysis

The mixed formulation presented in the previous section admits analytical solutions to within a numerically determined membrane force parameter. (7)–(9) together with the matching conditions, (16)–(23), and the pertinent boundary conditions of (15) and (24)–(27), can be readily solved to yield analytical solutions for the transverse displacement in terms of the membrane force. For given material and geometric properties, the membrane force can be evaluated numerically by substituting the corresponding analytical solutions into the integrability condition, (46), and finding roots (values of N_0) of the resulting transcendental equation using root solving techniques. Each root is associated with an equilibrium configuration of the evolving structure for given values of the temperature, pressure, damage size, and length of the contact zone. Once obtained, these values can be substituted back into the solution for the transverse deflection and the result then substituted into the transversality conditions (42) to generate the delamination growth paths for the evolving structure.[4] The onset, stability, and extent of propagation can be assessed from these paths. (As a special case, it may be noted from $(25)_2$ and $(41)_1$ that when the edges

---

[4]For computational purposes, it is often convenient to combine the equations of the integrability and transversality conditions in a strategic manner, depending upon the circumstances.

of the base structure are free to translate in the axial (circumferential) direction, the uniform membrane force vanishes identically ($N_0 \equiv 0$). For this case, the analytical solutions may be obtained by direct integration, and substituted into the transversality condition. The corresponding integrability condition will then simply yield the axial (circumferential) displacement of the edge of the base structure.) Finally, the issue of a propagating contact zone may be examined by evaluating a solution for a given value of b (associated with a given value of a) and checking to insure that the resulting displacements satisfy the kinematic inequality $(43)_2$. The energy release rates for configurations with valid contact zones may then be plotted as a function of the contact zone boundary coordinate, b, for selected values of the bond zone size, a. (It was shown in [Bottega 1995] that for a certain class of problems a propagating contact zone is not possible. Rather, if contact of the detached segment of the patch with the base structure is present it is either in the form of a full contact zone — that is, the entire debonded segment of the patch maintains sliding contact with the base structure — or edge point contact, where only the "free" edge of the patch maintains sliding contact [Karlsson and Bottega 1999b]. If, for this class, neither of these configurations is possible then contact does not occur: a contact zone does not exist.)

For the case of no contact zone, a relatively simple growth path can be determined in the load-bond zone boundary space and the deflection-bond zone boundary space, or equivalently in the load-deflection space. Various scenarios can be predicted from examination of these paths as follows. Consider the generic growth path shown in Figure 3, where λ represents the generalized "load", say the temperature change or the applied transverse pressure, and a^* corresponds to the size of the damaged region. For a given initial damage size (say point A, C, or F on the horizontal axis), no growth occurs as the load is increased until the load level is such that the growth path is intercepted. At that point growth ensues and may proceed according to several scenarios, depending upon the initial value of a^*. These scenarios include *stable growth* (BEH), where an increment in load produces an increment in damage size; *unstable growth* ($D \rightarrow E$) followed by stable growth (EH), where the damage propagates dynamically (that is, "jumps") to an alternate stable configuration and then proceeds in a stable manner thereafter; and unstable, *catastrophic growth* ($G \rightarrow H'$), where the damage propagates dynamically through the entire length of the patch, resulting in complete detachment of the patch from the base structure.
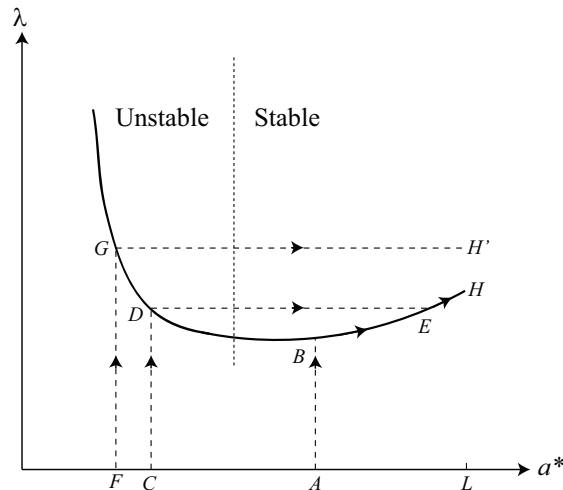

Figure 3. A generic debond growth path.

The formulation discussed in Section 2 and the procedure outlined in the current section are applied to examples of axially (circumferentially) unfettered structures in the next section.

5. Results for axially unfettered structures

In this section, we present results for structures that are completely unfettered and for those whose edges are free to translate in the axial (circumferential) direction. Specifically, in Section 5.1 we consider completely unfettered structures, flat or curved, subjected to temperature change alone. In Section 5.2 we consider the influence of temperature on edge debonding of both flat and curved structures subjected to three-point loading, and in Section 5.3 we examine the effects of temperature on the detachment of axially unfettered patched beam-plates subjected to transverse pressure.

5.1. *Unfettered structures in a uniform temperature field.*

In this section, we examine the behavior of structures, flat or curved, that are completely unfettered (that is, those whose edges are free). The results discussed also hold for the case of pinned-free supports. That is, for structures for which the edges of the base panel are free to translate with regard to axial (circumferential) translation and pinned with regard to rotation.

For this case, a free-body diagram of segments of the structure in each of the regions shows that

$$\kappa_1{}^* = \beta^*\Theta, \qquad \kappa_2{}^* = \kappa_3 = 0. \tag{50}$$

It follows from earlier discussions that for the present case passive contact occurs ($\kappa_2{}^* = 0$) for the entire detached segment of the patch, regardless of the sign of the thermally-induced curvature in the bond zone. In this case, the transversality conditions given by (42) reduce to the same form,

$$\mathcal{G} = \tfrac{1}{2}\big(\eta/\beta^{*2} - D^*\big)(\beta^*\Theta)^2 = 2\gamma. \tag{51}$$

Since the bond zone boundary does not appear explicitly in the equation (51) for the growth path, the energy release rate is independent of the location of the bond zone boundary. It follows that when growth occurs it is catastrophic. That is, when the critical temperature change is achieved, the entire patch detaches from the base structure in an unstable manner. Substitution of $(44)_2$, (13), and (14) into (51) renders the transversality condition for this case to the form

$$(\beta^*\Theta^*)^2 = \frac{2C_s h^{*2}}{D^*(4D^* - C_s h^{*2})}, \tag{52}$$

where

$$\Theta^* \equiv \Theta/\sqrt{2\gamma}. \tag{53}$$

It is seen from (52) that the critical renormed thermal curvature, $\beta^*\Theta^*$, is independent of the coefficients of thermal expansion of the constituent layers. The dependence of the critical thermal moment on the modulus ratio, E_0, is displayed in Figure 4 for the case $h_p = h = 0.05$. The peak value of the critical curvature occurs for $E_0 \simeq 0.25$. (For later reference, we note that for $E_0 = 1$, $\|\beta^*\Theta^*\|_{cr} = 0.8660$.) We remark that, during the thermal loading, deformation, and evolution processes, the entire debonded segment of the patch maintains sliding contact with the base structure regardless of the sign of the renormed thermal curvature, $\beta^*\Theta^*$.
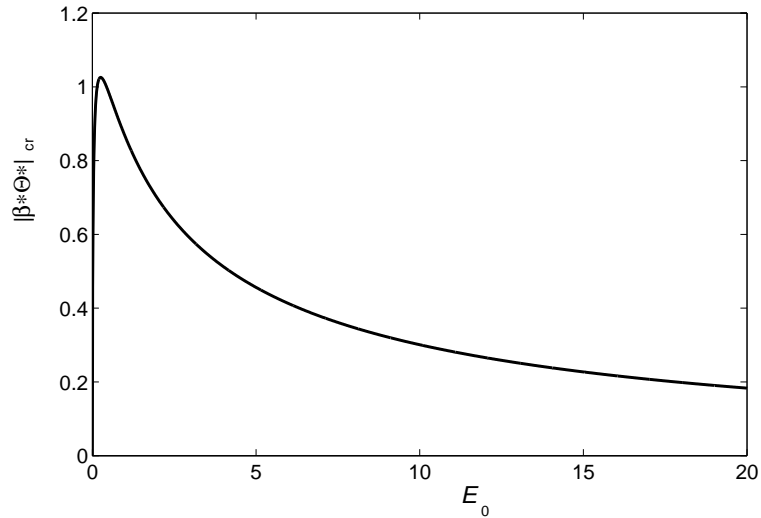
Figure 4. Critical renormed thermal curvature as a function of modulus ratio for a completely unfettered structure subjected to temperature change. ($h_p = h = 0.05$).

5.2. *Temperature change and three-point loading.* We next consider structures, both flat ($k = 0$) or cylindrical ($k = 1$), that are subjected to three-point loading and a uniform temperature field. For this case, the upwardly directed (normalized) transverse load at the center of the span is taken to be $2Q_0$, and the supports at the edges of the base panel are pinned-free. Equivalently, the edges of the base panel may each be considered to be loaded with a downwardly directed (normalized) transverse load Q_0 and the center of the span considered to be sitting on a knife edge (Figure 5). The normalized load, Q_0, is related to its dimensional counterpart, $\overline{Q}_0$, as follows:

$$Q_0 = \bar{Q}_0 \bar{\ell}^2 / \overline{D}, \tag{54}$$

where, as defined earlier, $\bar{\ell} = \overline{L}, \overline{R}$ (plate, shell). Consideration of the equilibrium of regions 2 and 3 of the structure shows that (43) is violated, and hence that no contact zone is present.

Patched plate. A region-wise moment balance for the patched beam-plate yields

$$\kappa_1{}^*(a) = \beta^*\Theta + \frac{Q_0}{D^*}(L - a), \qquad \kappa_3(a) = \frac{Q_0}{D}(L - a). \tag{55}$$
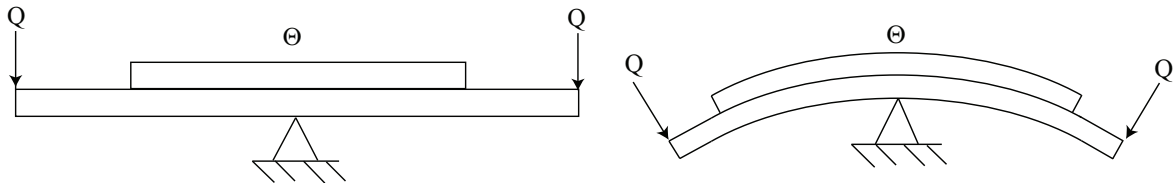

Figure 5. Three-point loading of patched structure. Left: patched beam-plate. Right: patched arch-shell.
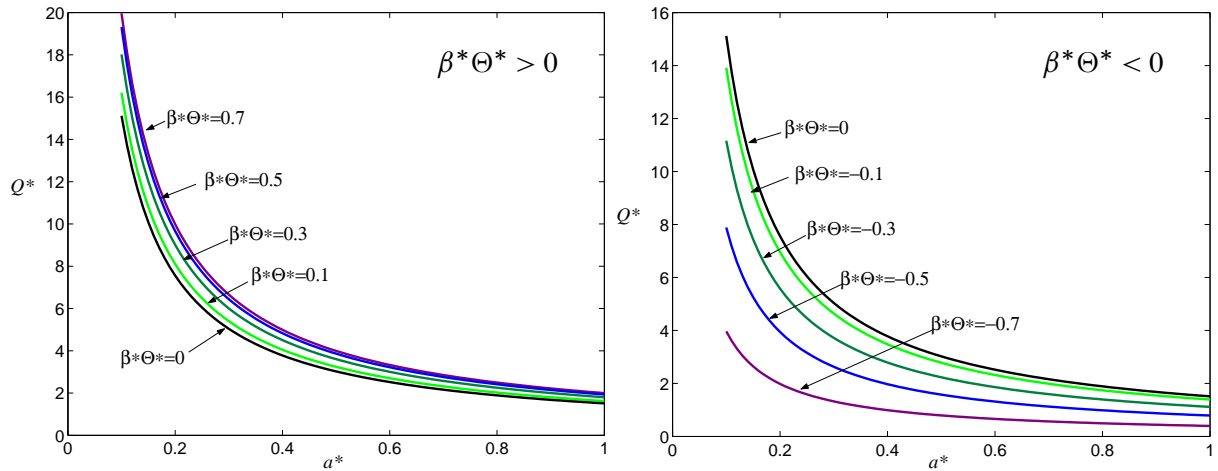
Figure 6. Growth paths for a patched plate subjected to three-point loading for various renormed temperatures (thermal curvatures). $\alpha_p/\alpha = 0.5$ or 2; $E_0 = 1$; $h = h_p = 0.05$.

It may be seen from these equations that a pseudo-inflection point may exist at $x = a$ when $\beta^*\Theta < 0$ and $\|\beta^*\Theta\| > Q_0(L-a)/D^*$. Substitution of (55) into $(42)_2$ reduces the transversality condition for the present case to the form

$$Q^{*2}a^{*2}\left(\frac{1}{D} - \frac{1}{D^*}\right) - 2Q^*a^*(\beta^*\Theta^*) + \left(\frac{\eta}{\beta^{*2}} - D^*\right)(\beta^*\Theta^*)^2 - 2 = 0, \tag{56}$$

where

$$Q^* \equiv Q/\sqrt{2\gamma}, \qquad \text{and} \qquad \Theta^* \equiv \Theta/\sqrt{2\gamma}. \tag{57}$$

The debond growth paths are easily generated from (56) for any structure of interest. Such paths are displayed in Figure 6 for a structure with the properties $E_0 = 1$, $h_p = h = 0.05$, $\alpha_p/\alpha = 0.5$, and $\alpha_p/\alpha = 2.0$. We note from Figure 4 that, for thermal loading alone, $\|\beta^*\Theta^*\|_{\text{cr}} = 0.8660$ when $E_0 = 1$. Thus, propagation will occur due to temperature change alone for this condition. To examine the effects of three-point loading we therefore consider temperature changes for which $\|\beta^*\Theta^*\|_{\text{cr}} < 0.8660$.

It may be seen from Figure 6 that, for any initial conjugate bond zone size, once the critical value of Q_0 is achieved it is sufficient for all larger conjugate bond zone sizes. Therefore, growth is catastrophic for all initial damage sizes. That is, once propagation ensues it continues unimpeded, with the patch ultimately completely separated from the base structure. To interpret these results further, we note the following. For the case $\alpha_p/\alpha = 2.0$, $\beta^* > 0$. Thus, for this case, the results displayed in Figure 6, left, correspond to positive temperature changes while those in Figure 6, right, correspond to negative temperature changes. For the case $\alpha_p/\alpha = 0.5$, $\beta^* < 0$, the interpretation is the reverse of that for $\alpha_p/\alpha = 2.0$. That is, for $\alpha_p/\alpha = 0.5$, the results shown on the left are associated with negative temperature changes while those on the right correspond to positive temperature changes. For negative thermally-induced curvature ($\beta^*\Theta^* < 0$), the intact segment of the composite structure is concave up, while the transverse load Q_0 tends to bend the detached segment concave downward thus encouraging "opening". In this way, the temperature changes are seen to encourage detachment (Figure 6, right), lowering the critical level of the

transverse load well below that for vanishing temperature, with increasing magnitude of the temperature change. In contrast, for positive thermally-induced curvature ($\beta^*\Theta^* > 0$), the intact segment of the composite structure is concave down in the same sense as the curvature change of the detached segment as induced by Q_0. The thermal effect here is to oppose "opening" and hence to resist detachment. In this sense, the critical level of the transverse load is seen to increase with increasing thermally-induced moment, as seen in Figure 6, left, though these effects are observed to be less dramatic than those associated with negative thermal moments.

Patched shell. We next consider the analogous problem of a patched panel subjected to three-point loading. Recall that for curved structures, length scales are normalized with respect to the *radius* of the undeformed structure. Normalized arc lengths are then angles. Proceeding as for the beam-plate, a region-wise moment balance for the patched panel yields

$$\kappa_1{}^*(a) = \beta^*\Theta + \frac{Q_0}{D^*}F(a), \qquad \kappa_3(a) = \frac{Q_0}{D}F(a), \tag{58}$$

where

$$F(a) = \cos L(\sin L - \sin a) + \sin L(\cos a - \cos L). \tag{59}$$

It is seen from the above equations that a pseudo-inflection point may exist at $x = a$ when $\beta^*\Theta < 0$ and $\|\beta^*\Theta\| > F(a)/D^*$. Substitution of (58) into the second line of (42) reduces the transversality condition for the present case to the form

$$Q^{*2}[F(a)]^2\left(\frac{1}{D} - \frac{1}{D^*}\right) - 2Q^*F(a)(\beta^*\Theta^*) + \left(\frac{\eta}{\beta^{*2}} - D^*\right)(\beta^*\Theta^*)^2 - 2 = 0, \tag{60}$$

where Q^* and Θ^* are defined by (57).

   For the purposes of comparison, we shall examine the behavior of a specific structure having the same proportions as those of the beam-plate considered earlier. Toward this end we consider the structure for which $L = 0.4$ radians, $h_p = h = 0.02$ (same thickness to length ratio as the plate), $E_0 = 1$ and $\alpha_p/\alpha = 0.5$ and 2.0. Corresponding results for a patched shell segment subjected to three-point loading (Figure 5, right) are displayed in Figure 7. It is seen that the behavior is very similar to that of the patched plate. (Recall that the load is normalized via (54).)

5.3. *Temperature change and transverse pressure.* In this section, we examine symmetric edge debonding of a patched beam-plate ($k = 0$) for cases where the edges of the base plate are free to translate in the axial direction. It follows from $(25)_2$ and (41) that, for these support conditions, $N_0 = 0$. This renders the governing differential equations for the transverse displacement $w(s)$, resulting from $(7)_1$, $(8)_1$, and $(9)_1$, linear. The solutions may thus be obtained by direct integration, with the constants of integration evaluated by imposing the boundary and matching conditions for transverse motion given by $(15a)_{2,3}$, (17), (18), (21)–(23), $(24)_{2,3}$, (26) and (27). We consider two extreme support conditions at the edges of the base plate: pinned-free and clamped-free. Based on these analytical solutions, numerical simulations are performed for structures possessing the representative properties $h_p = h = 0.05$, $E_0 = 1$, and $2\gamma = 0.1$. The first two properties render $B^* = \beta^* = 0$ and thus eliminate mechanical material bending-stretching coupling within the bonded region. We shall consider two complementary cases of
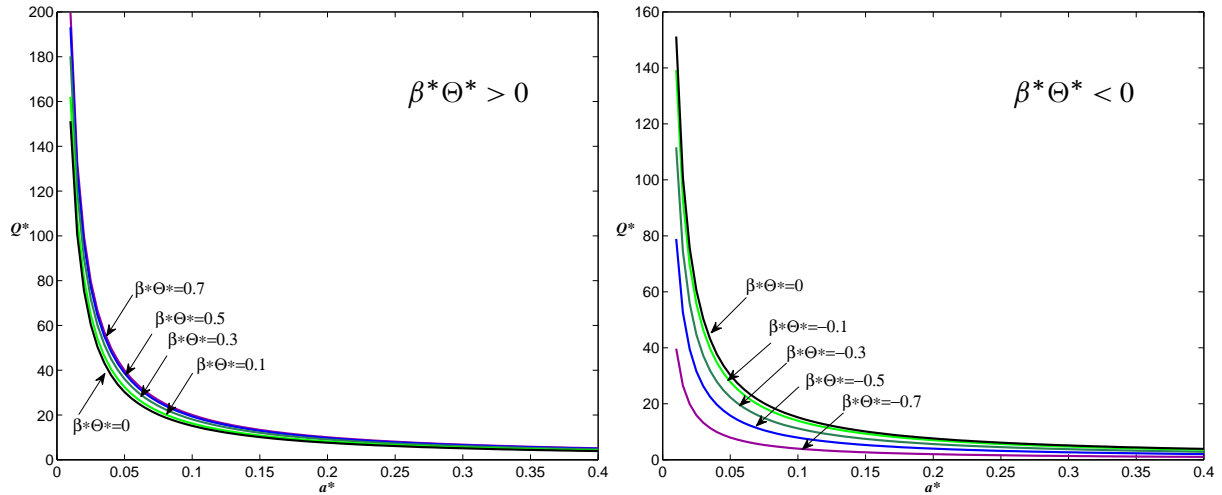
Figure 7. Growth paths for a patched shell subjected to three-point loading for various renormed temperatures (thermal curvatures). $\alpha_p/\alpha = 0.5$ or 2; $E_0 = 1$; $h = h_p = 0.02$; $L = 0.4$.

thermal mismatch: $\alpha_p/\alpha = 0.5$ and $\alpha_p/\alpha = 2.0$. For the purposes of presentation and interpretation of results, we introduce the characteristic deflection $\Delta_0 \equiv -w_1(0)$.

Hinged-free supports. We first examine the behavior of a structure with *hinged-free* supports. That is, a beam-plate for which the edges of the base-plate are hinged with respect to rotation and free with respect to in-plane translation (see Figure 1, left). For such support conditions, it may be anticipated that the deformed structure will not exhibit an inflection point or pseudo-inflection point, under the loading considered when deflections are upward. It follows, from the discussion preceding (45), that if a contact zone is present it will be a full contact zone. Moreover, a contact zone may be present only if the deflection of the structure is downward. However, for the supports and loading under consideration, the curvature of the bonded region will be concave upward during negative deflection, but the curvature of the base plate in the unpatched and detached regions will be concave downward regardless of the sign of the deflection. Thus, there will be a pseudo-inflection point at the bond zone boundary for downward deflections of the structure. Since the curvature of the patch in the detached region must be zero or concave upward, a contact zone is not possible.

Debond growth paths for the ratio $\alpha_p/\alpha = 0.5$ are displayed in Figure 8 for various values of the renormalized temperature $\tilde{\Theta} = \alpha\Theta$. The growth paths are presented in $p - a^*$ space (left half of the figure) and in $\Delta_0 - a^*$ space (right half).

For this ratio of thermal expansion coefficients, the influence of the temperature is greater for the base plate than for the patch, which results in a "concave up" curvature ($\beta^*\Theta < 0$) within the bond zone for positive temperature changes. This opposes the concave down curvature induced by the pressure and thus tends to "flatten" the structure within this region. In contrast, since the unbonded and debonded regions of the base plate are bent by the pressure alone, with the temperature change simply extending that segment of the structure, the curvature in these regions is concave downward. When the pressure
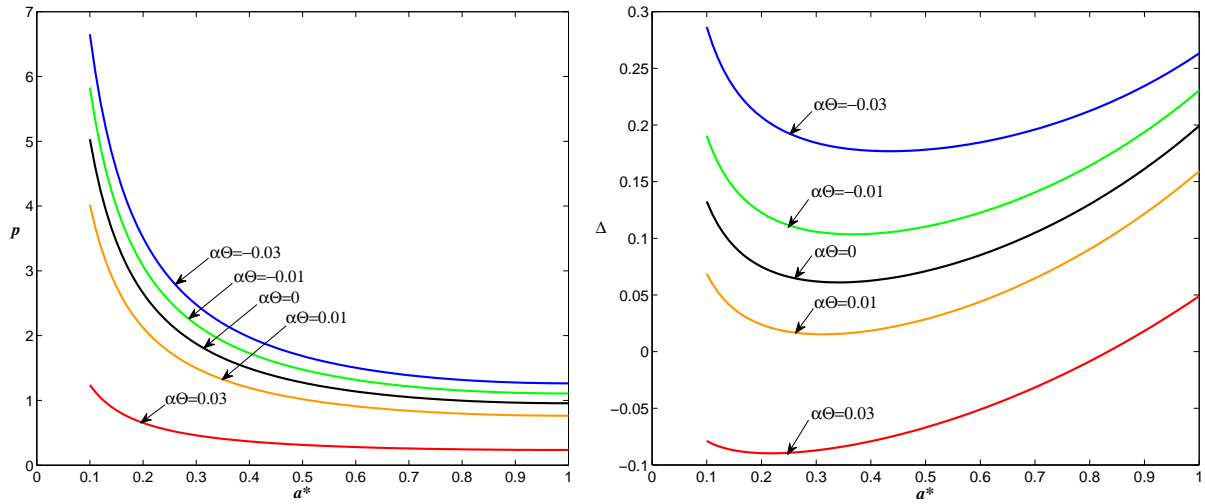
Figure 8. Debond growth paths for structures possessing hinged-free supports, with $\alpha_p/\alpha = 0.5$. Left: p versus a^*. Right: Δ_0 versus a^*.

effect dominates over the thermal moment, the curvature of the bond zone is concave down resulting in an upward deflection of the structure. For pressure-temperature combinations such that the deflection of the structure is upward, the "flattening" of the bond zone (by the temperature change) increases the relative bending of the unpatched segment of the base plate and hence the energy release rate for a given pressure, resulting in a lowering of the threshold pressure with increasing temperature change, as indicated. Moreover, when the temperature is sufficiently large such that the effects of the thermal moments dominate over those due to the pressure, then the curvature within the bond zone will be concave upward and the deflection of the structure will be downward. For these situations, the curvatures of the structure within the bonded and unbonded/debonded regions are of opposite sign, further increasing the relative bending between the detached and bonded segments at the bond zone boundary, and thus increasing the energy release rate at a given pressure level. This, in turn, results in further decreasing of the threshold pressure. Conversely, the threshold pressure increases with decreasing temperature. As the temperature change becomes negative, the thermal moment becomes positive ($\beta^*\Theta > 0$) and reinforces the mechanical moment rendering the curvature of the structure within the bond zone concave down — the same sense as within the detached/unbonded region. As a result, the relative bending at the bond zone boundary is reduced for a given value of the applied pressure and, consequently, the energy release rate. The threshold pressure, therefore, increases accordingly. In this sense, the effect of the thermal moment may be viewed as a reduction of the effective stiffness of the composite structure within the bonded region. At some point, the thermal effect reduces the "effective local stiffness" to the extent that the curvature of the structure within the bond zone is comparable with that of the detached segment of the base plate.

The debond growth paths for a mechanically and geometrically identical structure with $\alpha_p/\alpha = 2.0$ are displayed in Figure 9 for various values of the normalized temperature change. For ratios of the coefficients of thermal expansion greater than one, the thermal moment is positive ($\beta^*\Theta > 0$) for positive temperature changes. The scenarios for structures with this property are therefore the reverse of those for $\alpha_p/\alpha = 0.5$ discussed previously.
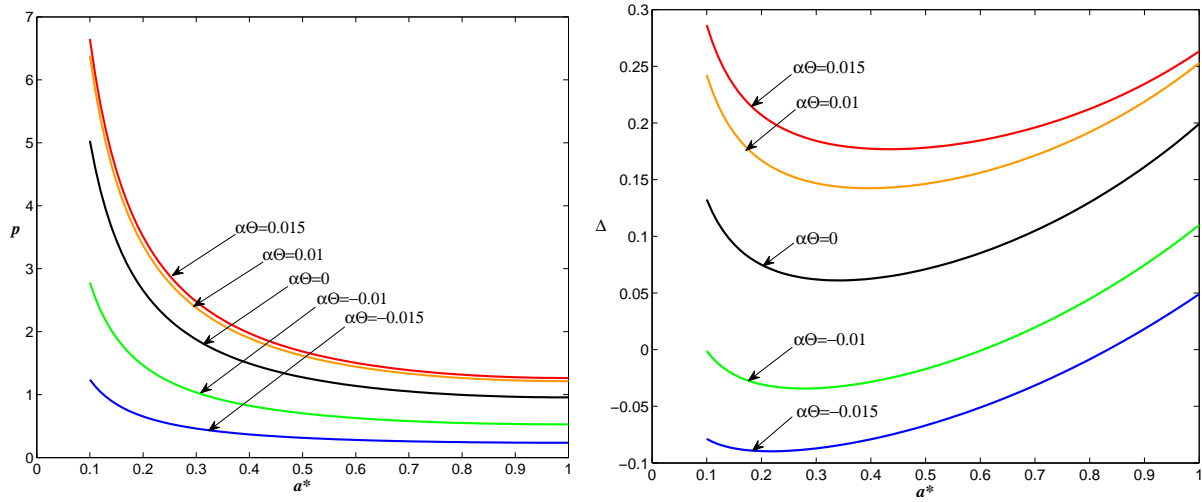
Figure 9. Debond growth paths for structures possessing hinged-free supports, with $\alpha_p/\alpha = 2.0$. Left: p versus a^*. Right: Δ_0 versus a^*.

Clamped-free supports. We next examine the behavior of a structure with *clamped-free* supports. That is, a beam-plate for which the edges of the base-plate are clamped with respect to rotation and free with respect to in-plane translation (see Figure 1, right). The arguments put forth when discussing the previous case, regarding the effects of the competition between the thermal and mechanical moments within the bond zone and their implications regarding curvature of the structure within that region, are paralleled for the present case. However, the constraints imposed on the rotations at the supports for the present case induce a pseudo-inflection point at the bond zone boundary and/or, at least, one inflection point along the half-span [0, 1] for the type of loading considered. For the purposes of the present argument, we consider one inflection or pseudo-inflection point to be present on the half-span. It follows that the curvature of the segment of the structure nearest the support will be concave up when the deflection of the structure is upward. In this light, we deduce the following possible configuration scenarios from (43) and (45). When the deflection is upward, a pseudo-inflection point at the edge of the bonded region or an inflection point within the bond zone will be accompanied by a full contact zone. However, if an inflection point occurs within the unpatched/detached region then it will be accompanied by, at most, contact of the free edge of the patch with the detached segment of the base plate ("edge-point contact"). Conversely, when the deflection is downward, the curvature of the unpatched region will be concave down. For this situation, no contact zone will be present when a pseudo-inflection point is present at the bond zone boundary or an inflection point occurs within the bonded region. A partial propagating contact zone will be present when an inflection point occurs within the detached region and $\Delta_0 < 0$. Situations in which more than one critical point occurs along the span may be considered individually using the criterion established in Section 2 and discussed further in Section 3.

Growth paths for vanishing temperature are presented in Figure 10. Growth paths for structures with the property $\alpha_p/\alpha = 0.5$ are presented in Figure 11, and those for which $\alpha_p/\alpha = 2.0$ are shown in Figure 12, for selected values of the renormed temperature change. It is found, for the geometry and material ratios considered, that a full contact zone is possible for structures for which $L_p \geq 0.79$, depending upon
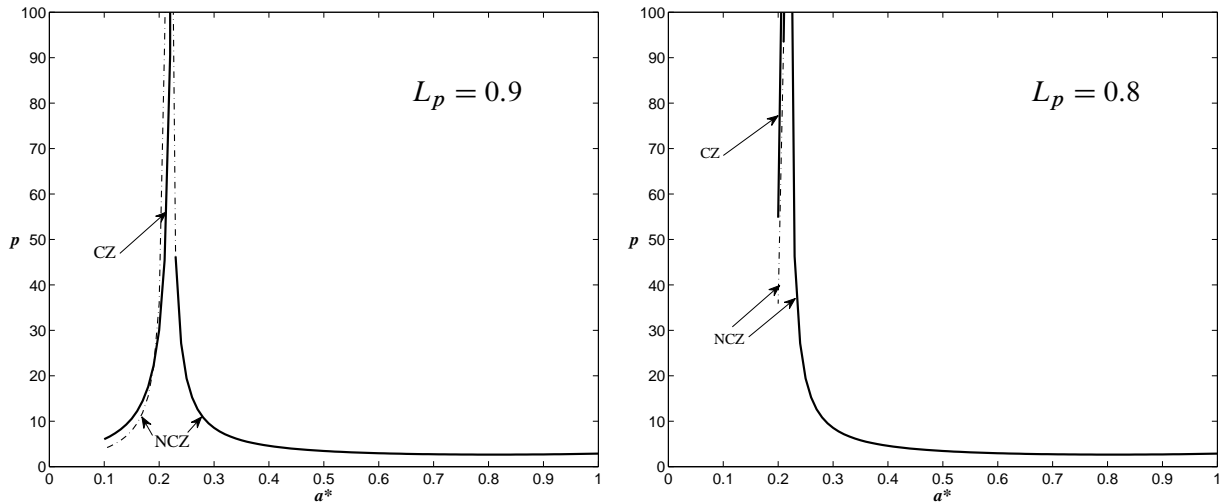
Figure 10. Contact zone (CZ) and no contact zone (NCZ) growth paths for structures subjected to pressure loading only ($\Theta = 0$) and possessing clamped-free supports.

the initial size of the damage. Structures possessing shorter patches have no contact zone regardless of the size of the damage.

Growth paths for a structure possessing a patch of length $L_p = 0.9$ for vanishing temperature change are presented in Figure 10, left. Those for a structure with a patch of length $L_p = 0.8$ are displayed in Figure 10, right. In these figures, the path labeled 'CZ' indicates the presence of a contact zone, and paths labeled 'NCZ' correspond to configurations with no contact zone. Invalid segments of the no contact paths are shown as dashed lines. Both legs of the NCZ path approach an asymptote at $a^* = 0.216$, while the CZ path for $L_p = 0.9$ approaches an asymptote at $a^* = 0.230$. It is seen that, when the contact zone is present, debonding is stable and that growth arrests as the asymptote is approached. It is also seen that the threshold values predicted with a contact zone present are lower than those predicted if it were neglected, for a range of values of a^*. For initial damage size to the right of the asymptote, growth is seen to be catastrophic for relatively small initial conjugate bond zone lengths, unstable followed by stable for intermediate initial damage sizes, and stable for relatively large initial conjugate bond zone sizes and/or patch half-lengths.

The effects of temperature are examined in Figures 11 and 12. The growth paths corresponding to selected temperature changes are displayed in p-a^* space and in Δ_0-a^* space in Figure 11 for structures where $\alpha_p/\alpha = 0.5$. In each case, dashed segments of the paths correspond to equilibrium configurations for which a contact zone is present, ($L_p = 0.9$), while solid lines indicate configurations with no contact zone. Upon consideration of the figures, it is seen that the qualitative debonding behavior under force-controlled loading for moderate to large flaw sizes is very similar to that previously discussed for structures with hinged-free support conditions, but shows slight stabilization for very large debonds. (This stabilization depends on the temperature, as stable debonding is recovered for smaller flaw sizes as the temperature increases.) For this range, no contact zone is present, $\Delta_0 > 0$, and an inflection point occurs in the unpatched/detached region. For long patches, a contact zone is present, reducing the relative bending at the bond zone boundary and thus raising the threshold pressure, stabilizing the process, and
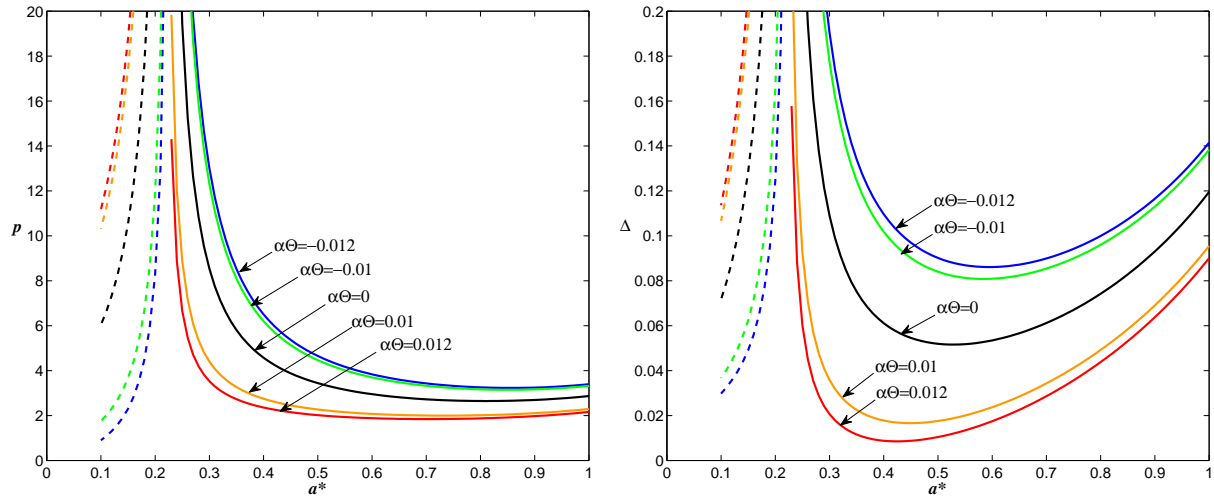
Figure 11. Growth paths corresponding to selected temperatures, for structures with clamped-free supports, with $\alpha_p/\alpha = 0.5$. Dashed lines indicate contact zone configurations for $L_p = 0.9$. Solid lines indicate no contact zone.

Figure 12. Growth paths corresponding to selected temperatures, for structures with clamped-free supports, with $\alpha_p/\alpha = 2.0$. Dashed lines indicate contact zone configurations for $L_p = 0.9$. Solid lines indicate no contact zone.
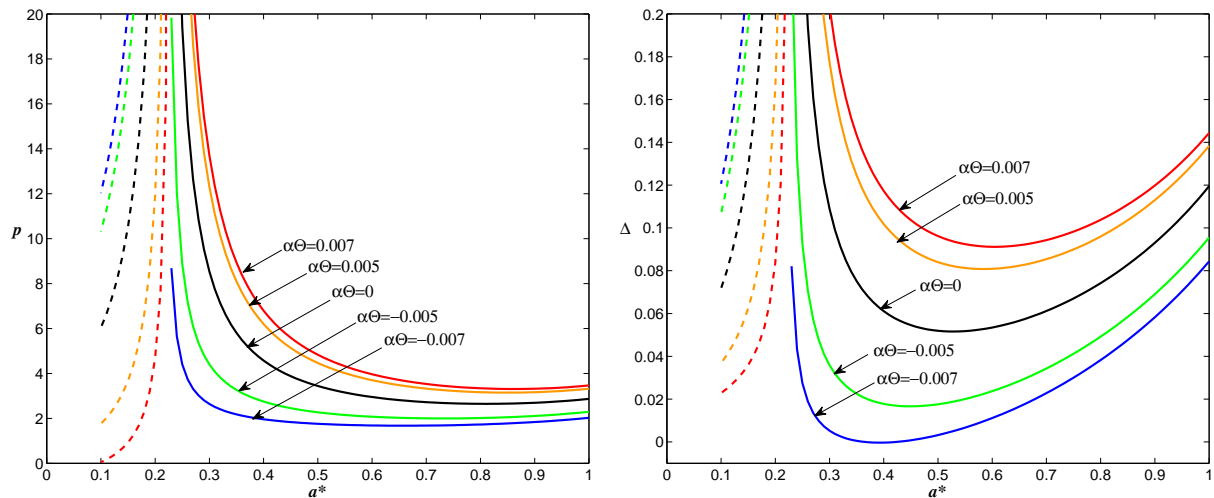
leading to eventual (asymptotic) arrest. The scenarios for deflection-controlled loading parallel those discussed for the hinged-free case, for moderate to large disbonds as well. For long patches with small initial debonds, stable growth and asymptotic arrest is indicated as for force-controlled loading. Similar results are shown in Figure 12 for structures with $\alpha_p/\alpha = 2.0$, but the effects of temperature are reversed.

Mode mix. Lastly, we examine the ratio of the mode-II energy release rate to the mode-I energy release rate using the structural scale decomposition presented in Section 3. Configurations for which a contact

Hinged-free support conditions				Clamped-free support conditions			
$\alpha_p/\alpha = 0.5$		$\alpha_p/\alpha = 2$		$\alpha_p/\alpha = 0.5$		$\alpha_p/\alpha = 2$	
$\tilde{\Theta}$	G_{II}/G_I	$\tilde{\Theta}$	G_{II}/G_I	$\tilde{\Theta}$	G_{II}/G_I	$\tilde{\Theta}$	G_{II}/G_I
-0.03	0.0019	-0.015	2.9389	-0.012	0.2488	-0.007	2.5102
-0.01	0.3059	-0.010	4.7497	-0.010	0.3059	-0.005	1.7409
0	0.7500	0	0.7500	0	0.7500	0	0.7500
0.01	1.7409	0.010	0.0870	0.010	1.7409	0.005	0.3059
0.03	27.939	0.015	0.0019	0.012	2.0822	0.007	0.1991

Table 1. Dependence of delamination mode ratio on temperature change for structures with hinged-free and clamped-free support conditions.

zone is present correspond to pure mode-II debonding ($G_{II}/G_I \to \infty$). For situations in which no contact zone is present, results for both hinged-free and clamped-free support conditions show that the mode partition ratio is independent of the debond size. Therefore, the qualitative debond scenarios for a given temperature discussed earlier are not altered due to the dependence of bond strength on mode mix, the exception being the comparison of contact zone and no contact zone configurations. The threshold levels for contact zone configurations will be relatively higher than indicated for a given temperature, since γ will be higher for pure mode-II. For either support condition considered, it is seen that when $\alpha_p/\alpha = 0.5$, the ratio increases with increasing temperature, and vice versa. The reverse is seen when $\alpha_p/\alpha = 2.0$. The dependence of G_{II}/G_I on $\tilde{\Theta} \equiv \alpha\Theta$ is summarized in Table 1.

6. Concluding remarks

The problem of debonding of patched panels subjected to temperature change and transverse pressure has been formulated from first principles as a propagating boundaries problem in the calculus of variations. This is done for both cylindrical and flat structures simultaneously. An appropriate geometrically nonlinear thin structure theory is incorporated for each of the primitive structures (base panel and patch) individually. The variational principle then yields the constitutive equations of the composite structure within the patched region and an adjacent contact zone, the corresponding equations of motion within each region of the structure, and the associated matching and boundary conditions for the structure. In addition, the transversality conditions associated with the propagating boundaries of the contact zone and bond zone are obtained directly, the latter giving rise to the energy release rates in self-consistent functional form for configurations in which a contact zone is present, as well as when it is absent. Further, a structural scale decomposition of the energy release rates is established by advancing earlier work of the first author to include the effects of temperature. The formulation is utilized to examine the behavior of several representative structures and loadings. These include debonding of completely unfettered patched structures subjected to temperature change, the effects of temperature on the detachment of beam-plates and arch-shells subjected to three-point loading, and the effects of temperature on damage propagation in beam-plates, with both hinged-free and clamped-free support conditions, subjected to transverse pressure. For the unfettered structures subjected to thermal load, the dependence of the critical thermal moment is

found as a function of the ratio of elastic moduli, E_0, for the patch and base structure. The critical moment is found to increase rapidly as the modulus ratio is increased, to a peak value for a modulus ratio about $E_0 = 0.25$, and then to decrease as the modulus ratio increases beyond this value. Damage propagation for both plate and shell structures subjected to three-point loading is seen to occur in a catastrophic manner once the critical load level is achieved. The critical load level is seen to be significantly influenced by the temperature field, especially for the shell structures. Similar qualitative behavior was seen for force-controlled loading of patched beam-plates subjected to transverse pressure and uniform temperature for the case of hinged-free support conditions. However, for displacement-controlled loading, debond propagation was seen to be stable, unstable followed by stable, or catastrophic, depending on the initial damage size and the temperature. For the case of clamped-free supports, a contact zone is present for very long patches for a limited range of damage sizes. For these situations, growth was seen to be stable, with minor propagation of the damaged region, and to lead to asymptotic arrest. For shorter patches, and for long patches with moderate to large initial damage, no contact zone was present. For these situations, propagation was seen to be catastrophic for moderately small initial damage or moderately large patch size, unstable followed by stable for still larger initial damage and stable for very large initial damage or small patch lengths. The threshold levels of the applied pressure and the stability of debond growth were seen to be strongly influenced by temperature for force-controlled loading. This behavior and its dependence on temperature was accentuated for displacement-controlled loading.

To close, we remark that the membrane force vanishes identically for the axially unfettered structures discussed in Section 5, thus nullifying the contributions of the geometric nonlinearities for these support configurations. It was shown in [Carabetta and Bottega 2008], however, that retention of geometric nonlinearities is essential to adequately model debonding phenomena in thin structures for configurations in which the membrane force does not vanish identically. This is so regardless of whether or not buckling is an issue. In this light, the formulation and analytical procedure developed in the present work (Sections 2–4) is a geometrically nonlinear one, designed to study debonding behavior in structures possessing such configurations. This includes the study of the interaction of thermally-induced buckling and debond propagation as well. Extensive work in this area is currently in progress and will be presented in a forthcoming article by the authors.

Dedication

It is with great pleasure and honor that we contribute this paper to this special issue of JoMMS dedicated to Professor George J. Simitses, a true gentleman and scholar.

References

[Bottega 1995] W. J. Bottega, "Separation failure in a class of bonded plates", *Compos. Struct.* **30**:3 (1995), 253–269.

[Bottega 2003] W. J. Bottega, "Structural scale decomposition of energy release rates for delamination propagation", *Int. J. Fract.* **122**:1–2 (2003), 89–100.

[Bottega 2006] W. J. Bottega, "Sling-shot buckling of composite structures under thermo-mechanical loading", *Int. J. Mech. Sci.* **48**:5 (2006), 568–578.

[Bottega and Karlsson 1999] W. J. Bottega and A. M. Karlsson, "On the detachment of step-tapered doublers, 1: Foundations", *Int. J. Solids Struct.* **36**:11 (1999), 1597–1623.

[Bottega and Loia 1996] W. J. Bottega and M. A. Loia, "Edge debonding in patched cylindrical panels", *Int. J. Solids Struct.* **33**:25 (1996), 3755–3777.

[Bottega and Loia 1997] W. J. Bottega and M. A. Loia, "Axisymmetric edge debonding in patched plates", *Int. J. Solids Struct.* **34**:18 (1997), 2255–2289.

[Carabetta and Bottega 2008] P. M. Carabetta and W. J. Bottega, "Effects of geometric nonlinearities on damage propagation in patched beam-plates subjected to pressure loading", *Int. J. Fract.* **152**:1 (2008), 51–62.

[Duong and Wang 2007] C. N. Duong and C. H. Wang, "Bond-line analysis at patch ends", Chapter 7, pp. 248–279 in *Composite repair: theory and design*, Elsevier, Amsterdam, 2007.

[Duong and Yu 2002] C. N. Duong and J. Yu, "An analytical estimate of thermal effects in a composite bonded repair: plane stress analysis", *Int. J. Solids Struct.* **39**:4 (2002), 1003–1014.

[Karlsson and Bottega 1999a] A. M. Karlsson and W. J. Bottega, "On the detachment of step-tapered doublers, 2: Evolution of pressure loaded structures", *Int. J. Solids Struct.* **36**:11 (1999), 1625–1651.

[Karlsson and Bottega 1999b] A. M. Karlsson and W. J. Bottega, "The presence of edge contact and its influence on the debonding of patched panels", *Int. J. Fract.* **96**:4 (1999), 381–406.

[Karlsson and Bottega 2000a] A. M. Karlsson and W. J. Bottega, "On thermal buckling of patched beam-plates", *Int. J. Solids Struct.* **37**:34 (2000), 4655–4690.

[Karlsson and Bottega 2000b] A. M. Karlsson and W. J. Bottega, "Thermo-mechanical response of patched plates", *AIAA J.* **38**:6 (2000), 1055–1062.

[Moore 2005] T. D. Moore, "Thermomechanical peeling in multilayer beams and plates: a solution from first principles", *Int. J. Solids Struct.* **42**:1 (2005), 271–285.

[Rose 1981] L. R. F. Rose, "An application of the inclusion analogy for bonded reinforcements", *Int. J. Solids Struct.* **17**:8 (1981), 827–838.

[Rutgerson and Bottega 2002] S. E. Rutgerson and W. J. Bottega, "Thermo-elastic buckling of layered shell segments", *Int. J. Solids Struct.* **39**:19 (2002), 4867–4887.

[Rutgerson and Bottega 2004] S. E. Rutgerson and W. J. Bottega, "Pre-limit-point buckling of multilayer cylindrical panels under pressure", *AIAA J.* **42**:6 (2004), 1272–1275.

[Timoshenko 1925] S. Timoshenko, "Analysis of bi-metal thermostats", *J. Opt. Soc. Am.* **11**:3 (1925), 233–255.

[Toya 1992] M. Toya, "On mode I and mode II energy release rates of an interface crack", *Int. J. Fract.* **56**:4 (1992), 345–352.

[Toya et al. 2005] M. Toya, M. Oda, A. Kado, and T. Saitoh, "Enegy release rates for an edge delamination of a laminated beam subjected to thermal gradient", *J. Appl. Mech.* (*ASME*) **72**:5 (2005), 658–665.

[Wang and Rose 2000] C. H. Wang and L. R. F. Rose, "Compact solutions for the corner singularity in bonded lap joints", *Int. J. Adhes. Adhes.* **20**:2 (2000), 145–154.

[Wang et al. 2000] C. H. Wang, L. R. F. Rose, R. Callinan, and A. A. Baker, "Thermal stresses in a plate with circular reinforcement", *Int. J. Solids Struct.* **37**:33 (2000), 4577–4599.

WILLIAM J. BOTTEGA: bottega@rci.rutgers.edu
Department of Mechanical and Aerospace Engineering, Rutgers University, 98 Brett Road, Piscataway, NJ 08854-8058, United States

PAMELA M. CARABETTA: pamc@eden.rutgers.edu
Department of Mechanical and Aerospace Engineering, Rutgers University, 98 Brett Road, Piscataway, NJ 08854-8058, United States